TSG-6 as a biomarker to predict efficacy of human mesenchymal stem/progenitor cells (hMSCs) in modulating sterile inflammation in vivo

Ryang Hwa Lee[a,1,2], Ji Min Yu[a,1], Andrea M. Foskett[a], Grant Peltier[a], John C. Reneau[a], Nikolay Bazhanov[a], Joo Youn Oh[b], and Darwin J. Prockop[a,2]

[a]Institute for Regenerative Medicine, Texas A&M Health Science Center College of Medicine at Scott and White, Temple, TX 76502; and [b]Department of Ophthalmology, Seoul National University Hospital, Jongno-gu, Seoul 110-744, Korea

Contributed by Darwin J. Prockop, August 20, 2014 (sent for review July 9, 2014)

Human mesenchymal stem/progenitor cells (hMSCs) from bone marrow and other tissues are currently being administered to large numbers of patients even though there are no biomarkers that accurately predict their efficacy in vivo. Using a mouse model of chemical injury of the cornea, we found that bone-marrow–derived hMSCs isolated from different donors varied widely in their efficacy in modulating sterile inflammation. Importantly, RT-PCR assays of hMSCs for the inflammation-modulating protein TSG-6 expressed by the TNFα-stimulated gene 6 (*TSG-6* or *TNFAIP6*) predicted their efficacy in sterile inflammation models for corneal injury, sterile peritonitis, and bleomycin-induced lung injury. In contrast, the levels of TSG-6 mRNA were negatively correlated with their potential for osteogenic differentiation in vitro and poorly correlated with other criteria for evaluating hMSCs. Also, a survey of a small cohort suggested that hMSCs from female donors compared with male donors more effectively suppressed sterile inflammation, expressed higher levels of *TSG-6*, and had slightly less osteogenic potential.

neutrophils | gender | myeloperoxidase | MPO

Human mesenchymal stem/progenitor cells (hMSCs) from bone marrow, adipose tissues, placenta, umbilical cord, and other tissues are currently being administered to large numbers of patients. Over 80 clinical trials with hMSCs have been registered (clinicaltrials.gov), and 5 have reached the Phase II or III stage of development (1). The trials are proceeding even though cultures of the cells are heterogeneous, and there is large variability in quality of hMSCs dependent on conditions, such as differences among donors, conditions used to expand the cells in culture, and random sampling in harvesting the cells from bone marrow and other tissues (2–5). Accounting for the variability among preparations is confounded by the lack of definitive markers for the cells. In addition, there are no biomarkers to predict the efficacy of hMSC samples in vivo. Therefore, the value of the data obtained from different clinical trials may well be compromised by variations in the quality of the hMSCs used.

Recent data suggest that the therapeutic effects of the cells were explained in part by their paracrine effects, such as expression of factors that modulate inflammatory and immune responses, that limit growth of cancers, or that enhance tissue repair (2, 6–8). We recently observed that i.v.-infused hMSCs modulated excessive sterile inflammation and thereby improved mouse models for myocardial infarction (9), corneal injury (10), or peritonitis (11), in part because the hMSCs were activated to secrete TNFα-stimulated gene 6 (TSG-6), a protein that is a natural modulator of inflammation (12–14). Of special interest was that a well-known model of chemical injury of the cornea made it possible to obtain quantitative dose–response data for the effectiveness of recombinant TSG-6 on both neutrophil infiltration and the functional integrity of the tissue (15). Using this model and two other models for sterile inflammation, here, we demonstrated that bone-marrow–derived hMSCs isolated from different donors showed wide variations in their efficacy in modulating inflammation. Also, we identified a biomarker of mRNA levels for TSG-6 that predicts the in vivo efficacy of different donor-derived hMSCs in suppressing inflammation. The biomarker should prove useful in selecting preparations of hMSCs for therapy of patients.

Results

We previously demonstrated (10) that, after ethanol injury and scraping of the cornea, i.v. infusion of bone-marrow hMSCs decreased sterile inflammation and thereby decreased opacity of the tissue. The hMSCs were effective even though quantitative PCR assays of mRNA for human GAPDH indicated that few if any of the cells reached the cornea after i.v. infusion of 10 million hMSCs in a similar rat model of ethanol injury of the cornea (10). As indicated in Fig. 1*A*, the decrease in opacity was proportional to the decrease in the cornea of myeloperoxidase (MPO), a semiquantitative measure of activated neutrophils. We used the same model to compare the efficacy of different preparations of hMSCs, here defined by the donors who provided the bone-marrow aspirates and expanded under essentially the same conditions, and found that they varied in their efficacy in suppressing opacity and MPO levels (Fig. 1 *B* and *C*). Some MSC preparations (from donors 235, 6015, and 269 of marrow aspirates) were highly effective, preventing opacity and decreasing MPO, and others (donors 7052, 7074, and 7075) provided little protection.

To identify a biomarker that predicted efficacy of hMSCs in the model, we assayed the same cells with conventional assays

Significance

The clinical trials with human mesenchymal stem/progenitor cells (hMSCs) from bone marrow and other tissues are proceeding even though cultures of the cells are heterogeneous and there is large variability among preparations of hMSCs due to differences among donors, culture conditions, and inconsistent tissue sampling. However, there is currently no in vitro bioassay for the evaluation of hMSC efficacy in vivo. Therefore, the value of the data obtained from current clinical trials may well be compromised by variations in the quality of the hMSCs used. This study provides, to our knowledge, the first biomarker that can predict the efficacy of hMSCs in suppressing sterile inflammation in vivo.

Author contributions: R.H.L., J.M.Y., and D.J.P. designed research; R.H.L., J.M.Y., A.M.F., G.P., J.C.R., and N.B. performed research; R.H.L., J.M.Y., A.M.F., G.P., J.C.R., and J.Y.O. analyzed data; and R.H.L., J.M.Y., and D.J.P. wrote the paper.

The authors declare no conflict of interest.

Freely available online through the PNAS open access option.

[1]R.H.L. and J.M.Y. contributed equally to this work.

[2]To whom correspondence may be addressed. Email: rlee@medicine.tamhsc.edu or Prockop@medicine.tamhsc.edu.

This article contains supporting information online at www.pnas.org/lookup/suppl/doi:10.1073/pnas.1416121111/-/DCSupplemental.

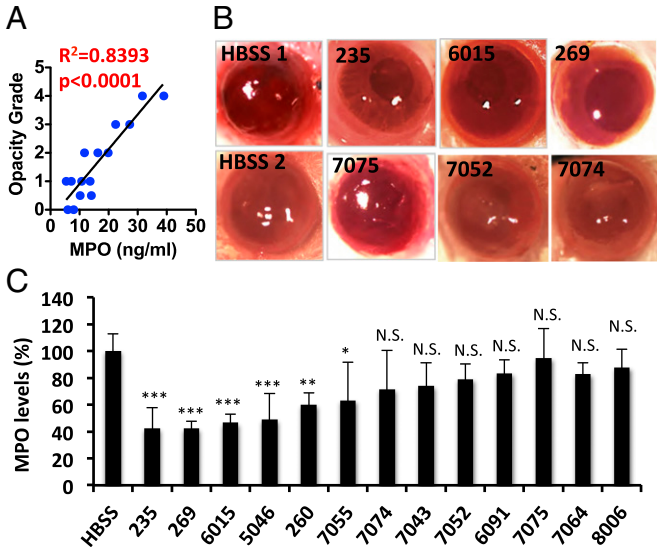

Fig. 1. hMSCs from different donors exhibit variations in therapeutic efficacy in suppressing sterile inflammation in the chemical burn-injured cornea. (*A*) Correlation between opacity grades and myeloperoxidase (MPO) levels in the cornea 3 d after ethanol injury and scraping of the epithelium. The values were data from 15 mice that were each treated with different numbers of hMSCs (0.01–1 × 10^6 cells) from donor 6015 or HBSS. (*B*) Representative corneal photographs on day 7 after injury and i.v. administration of vehicle (HBSS 1) or 1 × 10^6 hMSCs from different donors of bone-marrow aspirates. (*C*) Inflammation of the cornea as measured by MPO levels in the cornea on day 1 after injury. Values are means ± SD (n = 3–5 for each of 13 donor hMSCs; n = 6 for HBSS, *P < 0.05; **P < 0.01; ***P < 0.001; N.S., no significant difference; assessed by one-way ANOVA with Dunnett's multiple comparison test).

used to characterize MSCs in culture (16, 17). Surprisingly, there were no significant correlations with the efficacy of the cells in suppressing MPO in the model (Fig. 2*A*). In fact, there was a negative correlation with the potential of the hMSCs for osteogenic differentiation in vitro (Fig. 2*A*). Also, there was no significant correlation with adipogenic potential, rate of proliferation, and colony forming units-fibroblastoid (CFU-f). Similarly, there was no apparent relationship to the spindle-shaped morphology of cells (Fig. S1) that has been used to identify early progenitors in the cultures (18, 19), and there were no significant differences in expression of standard surface markers between the effective and ineffective hMSCs (Table S1).

To search further for informative biomarkers, we performed RT-PCR assays on the hMSCs for the expression of genes that have been suggested as responsible for anti-inflammation and immune-suppressive effects of hMSCs (6, 9–11, 20–24). As expected from previous observations in the cornea model (10, 15), there was a highly significant correlation between the levels of mRNA for TSG-6 in the hMSCs and their efficacy in reducing MPO levels in the cornea model (Fig. 2*B*). The correlation was essentially the same if based on assays of hMSCs that were freshly isolated from culture or on assays of the same cells after expression of *TSG-6* was increased by incubation with TNF-α for 16 h (9). There was a less-significant positive correlation with the levels of heme oxygenase 1 (HMOX1) in hMSCs that were freshly isolated from culture, but no significant correlation with hMSCs that were incubated with TNF-α. In addition, there were no significant correlations with the levels of mRNA for cyclooxygenase 2 (COX2), a key enzyme of synthesis of Prostaglandin E2, IL-1 receptor antagonist (IL-1Ra), transforming growth factor-β1 (TGF-β1), or indoleamine 2,3-dioxygenase 1 (IDO1).

The role of TSG-6 in the efficacy of the cells was confirmed by experiments (Fig. 3) in which *TSG-6* was overexpressed in hMSCs that initially expressed a low level of *TSG-6* (donor 7052). Overexpression of *TSG-6* decreased the potential of the cells to differentiate to mineralizing cells (Fig. 3*B*) and increased the efficacy of the hMSCs in the model for injury of the cornea (Fig. 3 *C*–*E*).

However, as hMSCs expressing high levels of *TSG-6* were expanded, there was a marked decrease in expression of *TSG-6* between 10 and 20 population doublings (Fig. S2). The results were consistent with previous observations that cultures of hMSCs lose many of their biological properties as they are expanded beyond about 20 population doublings in culture (17, 25).

To evaluate further the predictive value of *TSG-6* expression as a biomarker, we compared the efficacy of the hMSCs in two additional murine models: sterile inflammation of the peritoneum induced by zymosan (11) and lung injury induced by bleomycin (26). We tested six different donor preparations of hMSCs (Fig. 4*A*): three with the highest levels of *TSG-6* expression (defined as TSG-6^{hi} hMSCs) and three with the lowest levels (defined as TSG-6^{low} hMSCs). The efficacy of each of the six samples was then tested separately in the models.

As expected, the three preparations of TSG-6^{hi} hMSCs were more effective than the three preparations of TSG-6^{low} hMSCs in preventing opacity and decreasing MPO in the cornea model

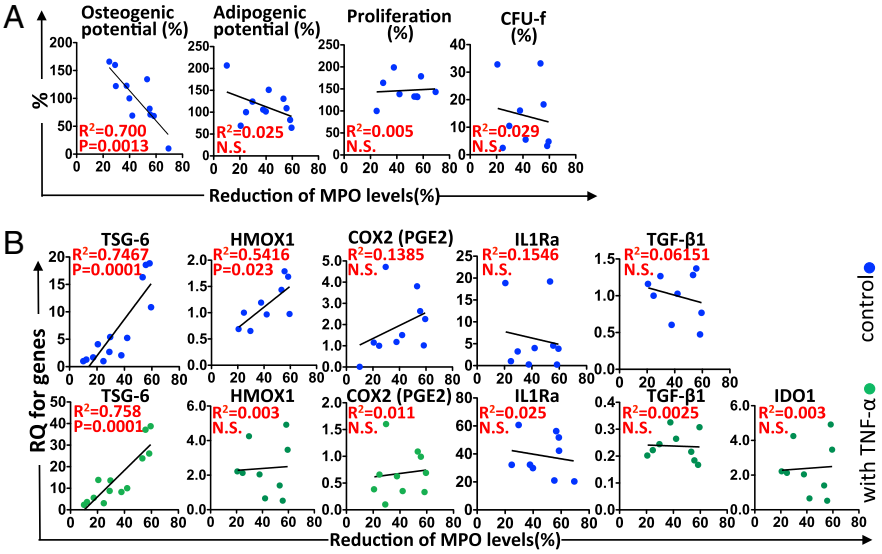

Fig. 2. Correlation between potential biomarkers and effectiveness in reducing MPO levels in the injured cornea. (*A*) Correlations between efficacy of hMSCs in reducing MPO levels in the cornea model and conventional assays in vitro for MSCs. (*B*) Correlations between efficacy of hMSCs in reducing MPO levels in the cornea model and expression by RT-PCR of genes previously linked to the therapeutic benefits of hMSCs. (*Upper* and *Lower*) Values obtained with (*Lower*) or without (*Upper*) stimulation of the cells with TNF-α. IDO1 was not detected in some hMSCs that were not stimulated with TNF-α.

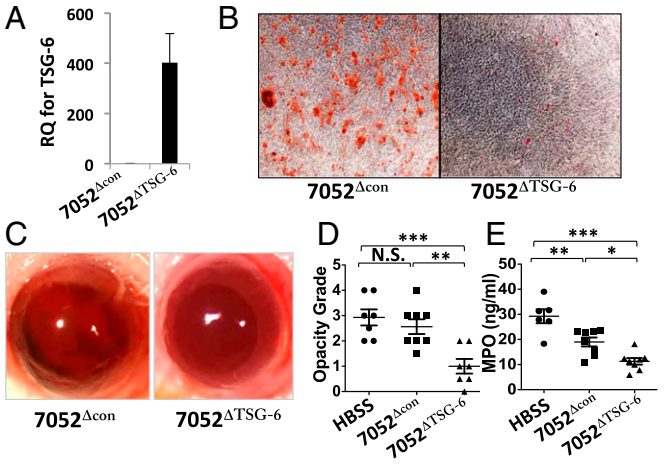

Fig. 3. Overexpression of *TSG-6* in hMSCs decreases osteogenic capacity in vitro and increases anti-inflammatory effects in vivo. (*A*) Real-time RT-PCR for the levels of *TSG-6* in hMSCs (donor 7052) transfected with control vector ($7052^{\Delta cont}$) or TSG-6 construct ($7052^{\Delta TSG\text{-}6}$) after 24 h. Values are means ± SD. (*B*) Representative photos of cultures of hMSCs stained with Alizarin Red after osteogenic differentiation. (*C*) Photographs of corneas of mice that received i.v. injections of 1×10^6 cells of $7052^{\Delta cont}$ or $7052^{\Delta TSG\text{-}6}$ after ethanol injury to cornea. (*D*) Quantification of corneal opacity on day 3 using clinical grading system on a 0–4 scale ($n = 7$ or 8 mice for each group, $^{**}P < 0.01$; $^{***}P < 0.001$; N.S., no significant difference; data evaluated by one-way ANOVA). (*E*) Inflammation of the cornea as assayed by MPO levels 1 d after the injury. The 7052 control MSCs were more effective in suppressing MPO levels than in Fig. 1*C*, apparently because transfection with control vector itself increased expression of *TSG-6* (not shown) (n = 6–8 for each group, $^{*}P < 0.05$, $^{**}P < 0.01$, $^{***}P < 0.001$; assessed by one-way ANOVA).

(Fig. 4 *B* and *C*). They were also more effective in reducing proinflammatory cytokines in the peritonitis model (Fig. 4*D*). In addition, in the bleomycin model for lung injury, in which fibrosis is detected by histology at 8 d (26), they were more effective in improving survival (Fig. 4*E*) and preserving body weight (Fig. S3*A*) in the treated mice compared with a control group. However, the differences in survival between mice that received TSG-6^{hi} hMSCs and TSG-6^{low} hMSCs were not significant because one (donors 265 and 7075) of each group showed moderate survival (Fig. S3*B*).

The negative correlation between efficacy in the cornea model and osteogenic potential of the hMSCs (Fig. 2*A*) raised the possibility that efficacy of the cells was linked to increased NF-κB signaling because a recent report indicated that increased NF-κB signaling inhibited osteogenesis (27). As expected, there was a negative correlation between osteogenic potential and expression of *TSG-6* in the hMSCs (Fig. 5*A*). Also, there was a weak correlation between expression of *TSG-6* and expression of *TNFRSF1A*, a tumor necrosis factor receptor superfamily member 1A, that may reflect the potential of TNF-α and other proinflammatory factors to up-regulate expression of TSG-6 (28). More importantly, NF-κB binding activity was higher in hMSCs expressing high levels of *TSG-6* (Fig. 5*C*), and inhibition of NF-κB signaling with SN50 (29) both decreased expression of *TSG-6* (Fig. 5*D*) and increased osteogenic differentiation of hMSCs in culture (Fig. 5 *E* and *F*).

To search for additional useful markers for hMSCs, we tested for correlations with the anonymous personal data available on the donors of the bone-marrow aspirates from which the hMSCs were obtained. Of special interest was that, in the small cohort available, expression of *TSG-6* has higher in hMSCs from female donors, especially after the cells were stimulated with TNF-α (Fig. 6*A*). Also, as expected, hMSCs from the female donors were more effective in suppressing MPO levels in the cornea model and had slightly less osteogenic potential in culture (Fig. 6*B*). There were negative correlations with height and weight

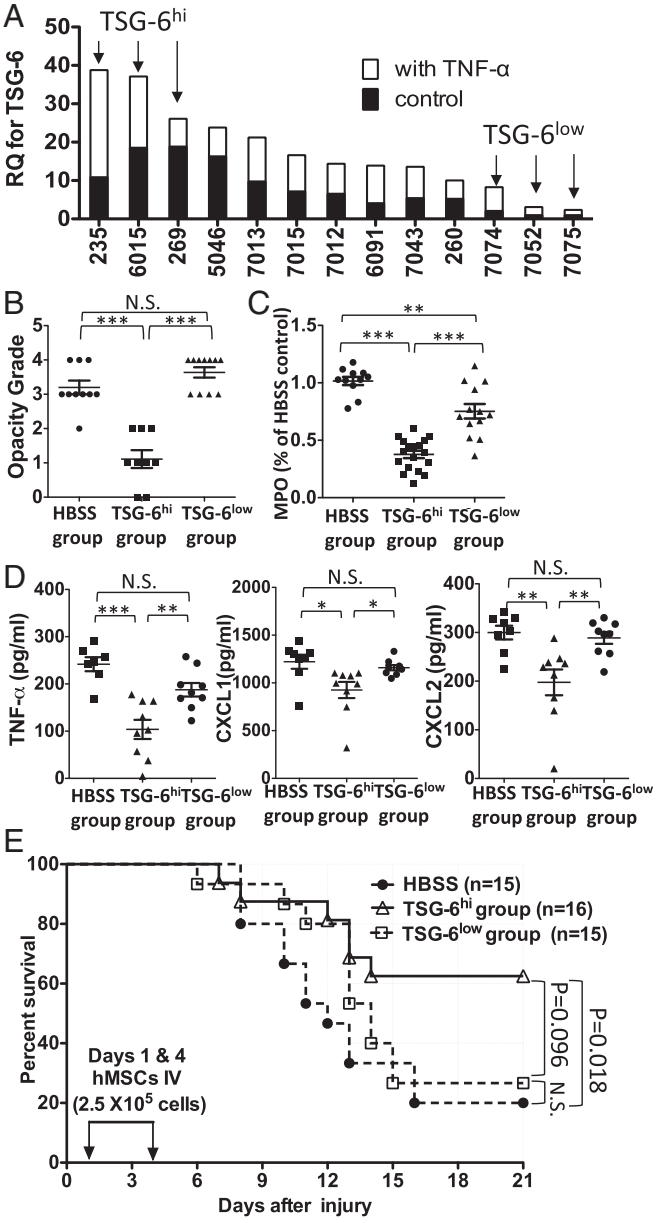

Fig. 4. The TSG-6^{hi} hMSCs are more effective in suppressing sterile inflammation in three in vivo models. (*A*) RT-PCR assays for *TSG-6* expression in hMSCs from a series of donors of bone-marrow aspirates with and without TNF-α stimulation. Values are relative to express level in donor 7075 that was set as 1.0. To simplify comparisons of the data from experiments in vivo, three preparations with the highest levels were designated as TSG-6^{hi}, and three with the lowest levels were designated as TSG-6^{low}. (*B*) Opacity of the cornea on day 7 after ethanol injury. The values are data from three to five mice that were each treated with hMSCs from the same six donors, of which three were TSG-6^{hi} hMSCs and three were TSG-6^{low} hMSCs ($^{***}P < 0.001$; N.S., no significant difference; assessed by one-way ANOVA). (*C*) Inflammation of the cornea 1 d after injury as assayed by MPO levels. ($n = 4$ or 5 mice that were treated with hMSCs from the same donor and $n = 12$ for HBSS control; $^{**}P < 0.01$, $^{***}P < 0.001$; assessed by one-way ANOVA). (*D*) Assays of the efficacy of the hMSCs in the mouse model for zymosan-induced peritonitis. Values are from ELISAs for mouse TNF-α, CXCL1, and CXCL2 in peritoneal lavage collected 4 h after i.p. injection of zymosan followed by injection of 1.5×10^6 hMSCs ($n = 3$ mice treated with the same donor MSCs and $n = 7$ for HBSS control; $^{*}P < 0.05$, $^{**}P < 0.01$, $^{***}P < 0.001$; N.S., no significant difference; assessed by one-way ANOVA). (*E*) Survival proportions after bleomycin injury of lung in mice followed by i.v. administration of 2.5×10^5 hMSCs [$n = 5$ or 6 mice treated with hMSCs from the same of six donors and $n = 15$ for HBSS controls; assessed by log-rank (Mantel-Cox) test].

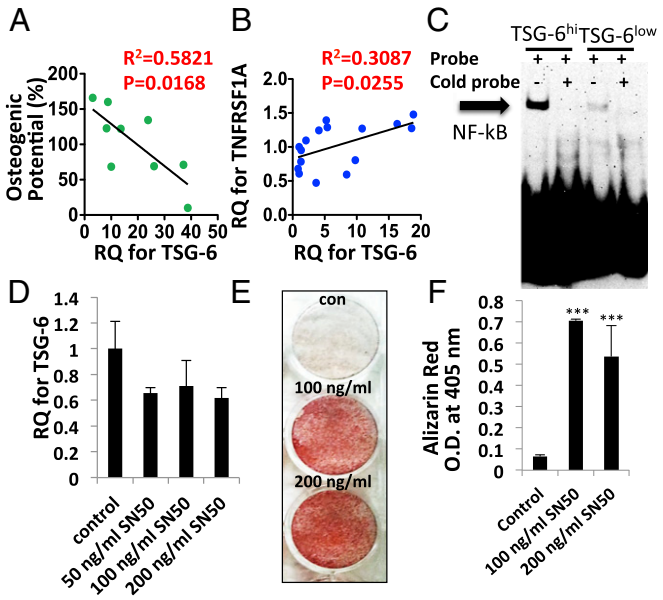

Fig. 5. Negative correlation between osteogenic differentiation potential and increased NF-κB signaling. (*A*) Correlation between osteogenic differentiation potential in vitro and the levels of mRNA for TSG-6 in hMSCs after stimulation with 5 ng/mL TNF-α stimulation for 16 h. (*B*) Correlation between the levels of mRNA for TSG-6 and TNFRSF1A in hMSCs. (*C*) Nuclear extracts from TSG-6^{hi} and TSG-6^{low} hMSCs were assayed for NF-κB DNA-binding activity by EMSA. The specific DNA-binding activity of NF-κB complex is indicated by an arrow. (*D*) Real-time RT-PCR for the levels of *TSG-6* in hMSCs (TSG-6^{hi} donor 6015) after 24-h treatment of SN50, an inhibitor of NF-κB signaling. Values are means ± SD. (*E*) Representative photo of cultures of TSG-6^{hi} hMSCs (donor 6015) treated with SN50, incubated in osteogenic medium, and stained with Alizarin Red. (*F*) Quantification of Alizarin Red staining of cultures treated as in *E*. Values are means ± SD (n = 3; ***P < 0.001; assessed by one-way ANOVA).

(Fig. 6*C*), but no correlation with age in the small cohort that was clustered in the younger ages (Fig. 6*C*). Adjusting for height and weight via a body mass index, analyses of the data with three subsequent multiple linear-regression models incorporating all of the above measures indicated that the most parsimonious models for *TSG-6* levels in hMSCs (with and without TNF-α stimulation) included a sex coefficient as the common predictive item. The MPO-level difference between females and males is highly significant (P = 0.0009); the 95% confidence interval for this difference indicated that male donors showed decreases in MPO levels that ranged from 7.06% to 40.07%, compared with female donors.

We also detected a negative correlation between date of collection of the bone-marrow aspirates from which hMSCs were immediately prepared and the efficacy of the cells in the cornea model (Fig. S4): i.e., the older samples were more efficacious. This correlation was probably explained by the fact that most of the older samples were from female donors and the more recent from male donors (Table S2).

To explore further the apparent sex bias, we examined the effects of incubating hMSCs with estradiol, the female hormone that reaches the highest peak values in serum (up to 1.6 nM) during the menstrual cycle (30). One-day exposure of hMSCs to low doses (10–100 pM) of estradiol decreased TSG-6 levels in hMSCs whereas a high dose (100 nM) of estradiol increased *TSG-6* expression in hMSCs (Fig. S5*A*). The effects of the high dose persisted after incubation with 100 nM for 2 d, in that the increased levels of TSG-6 mRNA were observed after the cells were incubated without estradiol for an additional 2 d (Fig. S5*B*). Furthermore, pretreatment of low doses of estradiol in hMSCs for 4 d promoted osteogenic differentiation whereas pretreatment with a high dose of 400 nM for 4 d suppressed osteogenic differentiation (Fig. S5 *D* and *E*), without affecting cell viability (Fig. S5*C*).

Discussion

The results presented here may overcome a major barrier to research with hMSCs: they provide, to our knowledge, the first biomarker that can predict the efficacy of the human cells in reducing sterile inflammation in in vivo models. Assays in the model for ethanol injury of the cornea demonstrated marked differences in the inflammation-suppressive efficacy of different preparations of hMSCs. The efficacy of the hMSCs, in turn, was proportional to their mRNA levels for the inflammation-modulating protein TSG-6. The levels of *TSG-6* expression predicted the efficacy of the cells not only in the model for chemical injury of the cornea but also for sterile inflammation produced by i.p. injection of the yeast extract zymosan in mice and, with somewhat less accuracy, in a more complex murine model of bleomycin-induced lung injury. The more variable results in the bleomycin model probably reflect the complexity of this model in which bleomycin triggers apoptosis and releases oxidants, and this injury followed first by a phase marked by invasion of inflammatory and immune cells and then by a fibrotic phase (31).

The RT-PCR assay for *TSG-6* expression that was used is robust, and it can be performed in about 4 h. As reported

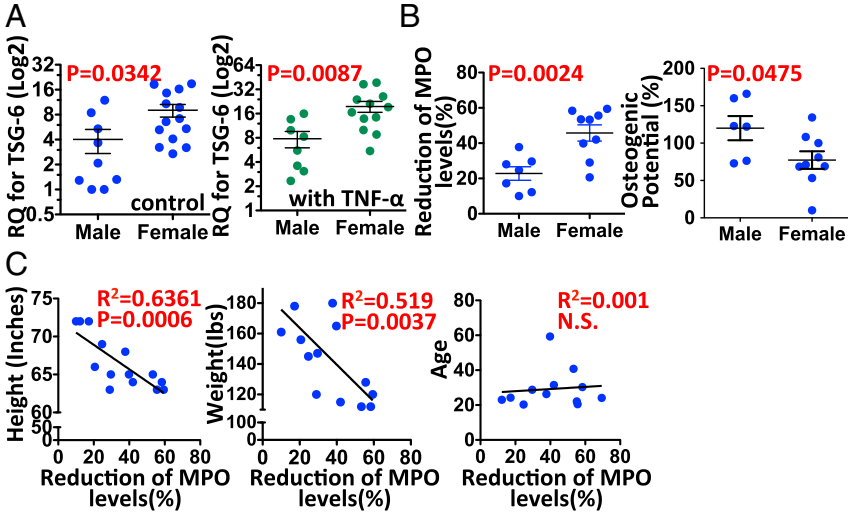

Fig. 6. Correlations with sex and other variables. (*A*) RT-PCR assays of TSG-6 in hMSCs from male and female donors of bone-marrow aspirates, with and without stimulation of the cells with TNF-α. (*B*) Comparison of hMSCs from male and female donors in reducing MPO in the model for ethanol injury of the cornea and in osteogenic potential in vitro. (*C*) Correlation of the efficacy of hMSCs in reducing MPO in the cornea model with height, weight, and age of donors.

previously (9), there was a close correlation between levels of mRNA for TSG-6 in MSCs and secretion of the protein in naive hMSCs, hMSCs stimulated with TNF-α, and knock-down experiments with siRNAs. Therefore, the levels of *TSG-6* expression with this assay, or some modified assay for *TSG-6* expression, should be useful in selecting hMSCs to reduce the variability in experiments and clinical trials with MSCs for the large number of diseases in which sterile inflammation is now recognized to play a critical role (3, 9, 32, 33). hMSCs, however, are highly sensitive to their microenvironments (3, 4, 9, 17, 25), and the levels of TSG-6 in a given preparation of MSCs may vary under different culture conditions to prepare the cells before administration in vivo.

One of the critical observations was that the conventional assays used to characterize hMSCs did not predict the efficacy of the cells in suppressing inflammation in vivo. Also, with the exception of heme oxygenase 1, there was no significant correlation with expression of several other genes previously linked to the therapeutic potentials of the cells (6, 9–11, 20–24). Of special interest was the negative correlation between the effectiveness of the cells in suppressing inflammation in the cornea model and their potential for osteogenic differentiation in culture because this negative correlation was linked to increased NF-κB signaling in the more efficacious cells and provided an independent marker for such cells. Also, the negative correlation with osteogenic differentiation suggests that hMSCs optimal for one application, such as suppression of inflammation, may be suboptimal for other applications, such as bone engineering. The decrease in *TSG-6* expression between 10 and 20 populations doubling suggests that the extensively expanded MSCs from a single "universal donor" may decrease the effectiveness of the cells in suppressing sterile inflammation.

The use of *TSG-6* expression as a biomarker for the efficacy of hMSCs in suppressing inflammation in vivo is consistent with previous observations on the protein (10, 12–15). TSG-6 is a naturally occurring protein of 35 kDa that is secreted by most cells in response to proinflammatory cytokines, and it has multiple actions that are linked to modulation of inflammation and stabilization of the extracellular matrix (12–14). Among its multiple actions is that TSG-6, either directly or through a complex with hyaluronan, binds to CD44 on resident macrophages in a manner that decreases TLR/NF-κB signaling and modulates the initial phase of the inflammatory response of most tissues (11, 20). hMSCs were observed to lose their effectiveness in several animal models for human diseases after siRNAs were used to knock down expression of *TSG-6* (9–11, 20, 34). Also, administration of recombinant TSG-6 reproduced most of the beneficial effects of the hMSCs (9–11, 20, 34). The role of TSG-6 in the cornea model was further validated here by the demonstration that overexpression of *TSG-6* greatly enhanced the effectiveness of hMSCs. However, the data to date have not established that TSG-6 is the only paracrine factor secreted by MSCs that suppresses inflammation, and it is possible that genes expressed upstream of *TSG-6* may prove to be useful biomarkers.

Surprisingly, comparison of hMSCs from a small cohort suggested that hMSCs from female donors compared with male donors were more effective in suppressing inflammation in the cornea model, expressed higher levels of *TSG-6*, and had slightly less potential for osteogenic differentiation. The data suggesting a sex bias in donors of hMSCs is consistent with a large body of literature demonstrating marked differences in susceptibility to diseases between men and women (35) and the effects of menstrual cycles on women (36, 37).

The use of *TSG-6* expression as a biomarker should improve selection of the most effective MSCs for clinical trials and overcome some of the variations in patient responses.

Materials and Methods

Cell Preparations. hMSCs were prepared from bone-marrow aspirates under the Institutional Biosafety Committee as previously described (9, 11). The aspirates were obtained under institutional review board approved protocols over several years from normal volunteers who responded to local postings in an academic setting (Table S2) and who were screened beforehand with blood assays for infectious agents. In brief, mononuclear cells were isolated by ficoll gradient separation of bone-marrow aspirates from the iliac crest of normal volunteers, incubated in complete culture medium (CCM) [α-MEM (Life Technologies) containing 17% (vol/vol) FBS (Atlanta Biologicals), 2 mM L-glutamine, and 1% (vol/vol) penicillin–streptomycin (Life Technologies)] at high density to obtain adherent cells (P0 cells), replated at low density (60–100 cells per cm^2), incubated to about 70% confluency (cell density about 10,000 cells per cm^2 at harvest), and frozen (P1 cells, 1×10^6 cells per vial). Frozen vials of P1 cells were thawed and incubated at high density for 24 h to obtain adherent viable cells, replated at low density (200 cells per cm^2), and incubated to about 70% confluency (cell density about 10,000 cells per cm^2 at harvest) to obtain P2 hMSCs that we used for the experiments. Population doublings were estimated as an average of five doublings (50-fold increase in cell number) per passage.

To activate the cells to express TSG-6, P2 hMSCs were incubated with 5 ng/mL TNF-α (R&D Systems) in α-MEM containing 2% FBS for 16 h (9). Similar results were obtained with two or more vials of P1 hMSCs from the same master bank prepared from the same donor. The FBS used for the experiments was selected by screening four to five lots for rapid growth of hMSCs. Different lots standardized to provide about the same propagation rate of hMSCs were used to prepare P0 hMSCs, but the same lot was used to expand P1-to-P2 hMSCs for the experiments here.

RNA Extraction from Cultured Cells and Real-Time RT-PCR Analysis. Total RNA from monolayer cells was extracted (RNeasy Mini kit; Qiagen), and about 0.1–1 μg of total RNA per sample was used to synthesize double-stranded cDNA by reverse transcription (SuperScript III; Life Technologies). Real-time RT-PCR was performed in triplicate for human *GAPDH, TSG-6 (TNFAIP6), HMOX1, COX2, IL1Ra, TGF-β1, IDO1,* and *TNFRSF1A*, using TaqMan Gene Expression Assays (Life Technologies). Real-time amplification was performed with TaqMan Universal PCR Master Mix (Life Technologies) and analyzed on a 7900HT fast real-time PCR system (Life Technologies). For assays, reactions were incubated at 50 °C for 2 min, 95 °C for 10 min, and then 40 cycles at 95 °C for 15 s, followed by 60 °C for 1 min. Data were analyzed with Sequence Detection Software, version 2.3 (Life Technologies), and relative quantities (RQs) were calculated with the comparative CT method using RQ Manager, version 1.2 (Life Technologies).

Animals. The experimental protocols were approved by the Institutional Animal Care and Use Committee of the Texas A&M Health Science Center. Six- to seven-week-old male BALB/c mice (BALB/cAnNCrl; Charles River Laboratories International) were used in all experiments.

Animal Model of Corneal Injury and Treatment. Chemical burned corneal injury was produced as described previously (15). Mice were anesthetized by isoflurane inhalation. To create the chemical burn, 100% ethanol (Sigma-Aldrich) was applied to the whole cornea, including the limbus, for 30 s, followed by rinsing with 1 mL of PBS (Life Technologies). Then, the epithelium over the whole corneal and limbal region was mechanically scraped using a surgical blade. Upon completion of the procedure, the eyelids of a mice were closed with one 8-0 silk suture at the lateral third of the lid margin. Immediately after injury, mice received i.v. injection of hMSCs (1×10^6) in 0.1 mL of Hanks' balanced salt solution (HBSS; Life Technologies).

Ocular Surface Evaluation. After injury and treatment, the mouse corneas were examined for corneal opacity and photographed at 3 d or 7 d. Corneal opacity was assessed and graded as described previously from the photographs by an ophthalmologist who was not aware of the treatment of the mice (15).

Protein Extraction from Cornea. Corneas were excised by cutting just beyond the limbus, the interior surface was scraped with a small sponge to remove endothelial cells and iris, and then the corneas were cooled with liquid nitrogen. A 3-mm punch was used to obtain a sample from the center of each cornea that was lysed in 150 μL of tissue-extraction reagent containing protease inhibitors (Life Technologies). The samples were sonicated on ice and centrifuged at $15,000 \times g$ at 4 °C for 15 min. The supernatant was used for MPO ELISAs.

Mouse Model of Peritonitis and Measurements of Inflammation. To induce inflammation in male BALB/c mice, 1 mL of zymosan solution (1 mg/mL; Sigma-Aldrich) was administered by i.p, followed by i.p. injection of 1.5×10^6 each donor-derived hMSCs 15 min later (11). After 4 h, inflammatory exudates

were collected by peritoneal lavage, and the cell-free supernatant was used to measure levels of the proinflammatory molecules [mouse Tumor necrosis factor alpha (mTNFα), mouse chemokine (C-X-C motif) ligand 1 (mCXCL1), mouse Chemokine (C-X-C motif) ligand 2 (mCXCL2)] by ELISAs.

Mouse Model of Lung Injury Induced with Bleomycin. Lung injury was induced in female C57BL/6J mice anesthetized with isoflurane by administration of bleomycin sulfate (Sigma-Aldrich) at 2.25 U/kg of body weight in 0.9% sodium chloride via an intubation technique (26). Sham animals were given 0.9% sodium chloride alone. Intravenous administration of each donor-derived hMSCs (2.5×10^5 cells in 150 μL) was performed on days 1 and 4 postinjury. A portable mouse pulse oximeter (STARR Life Sciences Corp.) was used to monitor arterial blood oxygen saturation (SpO_2) in free-roaming nonanesthetized mice. Weight and SpO_2 measurements were recorded every other day for the entire duration of the 21-d survival study.

ELISAs. Mouse MPO (mouse MPO ELISA kit; HyCult Biotech), TNF-α, CXCL1, and CXCL2 (R&D Systems) were detected with commercially available ELISA kits following procedures described by the manufacturers.

TSG-6 Overexpression. To prepare TSG-6 cDNA, total RNA was isolated from hMSCs that were stimulated by incubation with 5 ng/mL TNF-α in α-MEM containing 2% FBS overnight (9). About 1 μg of total RNA was used to produce the first-strand cDNA pool by Reverse Transcriptase (Superscript II/oligo dT12-18; Life Technologies). cDNAs encoding human *TSG-6* (GenBank accession no. NM_007115) was amplified by PCR using the following primers: 5′-CGGGGTACCATGATCATCTTAATTTACTT-3′ (sense for hTSG-6), and 5′-GGTGATCAGTGGCTAAATCTTCCA-3′ (antisense for hTSG-6-WT). The PCR products were subcloned into the BamHI and EcoRI sites in multicloning sites of a pEF4-Myc/His plasmid (Life Technologies), and the plasmids were amplified in *Escherichia coli* DH5α cells (Life Technologies). The TSG-6 or control plasmid (0.1 μg per well in six wells) was transfected into hMSC with Lipofectamine 2000 (Life Technologies) according to the manufacturer's protocol. Twenty-four hours after transfection, the cells were harvested for assays.

Differentiation Assay. For details on the differentiation assay, see *SI Materials and Methods*.

Nuclear Extraction and NF-κB Electrophoretic Mobility-Shift Assay. Cells were harvested at a density of 10,000 cells per cm^2, nuclear fraction was extracted (Nuclear Extraction Kit; Signosis), and assays for nuclear NF-κB were performed using EMSA Kit (Signosis) according to the manufacturer's instructions.

Inhibition of NF-κB Signaling. hMSCs were plated at 10,000 per well in CCM in six-well plates. To inhibit NF-κB signaling, cells were treated with the NF-κB inhibitor SN50 (EMD Millipore) in CCM every 2 d for 4 d. Then, the medium was changed to osteogenic differentiation media. For RT-PCR, cells were treated with SN50 (50–200 ng/mL) for 24 h in CCM and harvested for RNA extraction.

Statistical Analyses. Comparisons between two groups were made with the use of unpaired and two-tailed Student *t* tests. Comparisons of more than two groups were evaluated by ANOVA. Survival of mice between groups was compared using a log-rank (Mantel–Cox) test. $P < 0.05$ was considered significant.

ACKNOWLEDGMENTS. We thank Prof. Takamaru Ashikaga (College of Engineering and Material Sciences, University of Vermont) for biostatistical evaluation of the data. The work was supported in part by NIH Grant P40OD011050 and a grant from the Cancer Prevention and Research Institute of Texas.

1. Syed BA, Evans JB (2013) Stem cell therapy market. *Nat Rev Drug Discov* 12(3):185–186.
2. Keating A (2012) Mesenchymal stromal cells: New directions. *Cell Stem Cell* 10(6): 709–716.
3. Prockop DJ, Oh JY (2012) Mesenchymal stem/stromal cells (MSCs): Role as guardians of inflammation. *Mol Ther* 20(1):14–20.
4. Phinney DG, et al. (1999) Donor variation in the growth properties and osteogenic potential of human marrow stromal cells. *J Cell Biochem* 75(3):424–436.
5. Huang S, et al. (2013) Dissimilar characteristics of umbilical cord mesenchymal stem cells from donors of different ages. *Cell Tissue Bank* 14(4):707–713.
6. Lee RH, Oh JY, Choi H, Bazhanov N (2011) Therapeutic factors secreted by mesenchymal stromal cells and tissue repair. *J Cell Biochem* 112(11):3073–3078.
7. Prockop DJ, Oh JY (2012) Medical therapies with adult stem/progenitor cells (MSCs): A backward journey from dramatic results in vivo to the cellular and molecular explanations. *J Cell Biochem* 113(5):1460–1469.
8. Bernardo ME, Fibbe WE (2013) Mesenchymal stromal cells: Sensors and switchers of inflammation. *Cell Stem Cell* 13(4):392–402.
9. Lee RH, et al. (2009) Intravenous hMSCs improve myocardial infarction in mice because cells embolized in lung are activated to secrete the anti-inflammatory protein TSG-6. *Cell Stem Cell* 5(1):54–63.
10. Roddy GW, et al. (2011) Action at a distance: Systemically administered adult stem/progenitor cells (MSCs) reduce inflammatory damage to the cornea without engraftment and primarily by secretion of TNF-α stimulated gene/protein 6. *Stem Cells* 29(10):1572–1579.
11. Choi H, Lee RH, Bazhanov N, Oh JY, Prockop DJ (2011) Anti-inflammatory protein TSG-6 secreted by activated MSCs attenuates zymosan-induced mouse peritonitis by decreasing TLR2/NF-κB signaling in resident macrophages. *Blood* 118(2):330–338.
12. Wisniewski HG, Vilcek J (1997) TSG-6: An IL-1/TNF-inducible protein with anti-inflammatory activity. *Cytokine Growth Factor Rev* 8(2):143–156.
13. Milner CM, Day AJ (2003) TSG-6: A multifunctional protein associated with inflammation. *J Cell Sci* 116(Pt 10):1863–1873.
14. Wisniewski HG, Snitkin ES, Mindrescu C, Sweet MH, Vilcek J (2005) TSG-6 protein binding to glycosaminoglycans: Formation of stable complexes with hyaluronan and binding to chondroitin sulfates. *J Biol Chem* 280(15):14476–14484.
15. Oh JY, et al. (2010) Anti-inflammatory protein TSG-6 reduces inflammatory damage to the cornea following chemical and mechanical injury. *Proc Natl Acad Sci USA* 107(39):16875–16880.
16. Sekiya I, et al. (2002) Expansion of human adult stem cells from bone marrow stroma: Conditions that maximize the yields of early progenitors and evaluate their quality. *Stem Cells* 20(6):530–541.
17. Digirolamo CM, et al. (1999) Propagation and senescence of human marrow stromal cells in culture: A simple colony-forming assay identifies samples with the greatest potential to propagate and differentiate. *Br J Haematol* 107(2):275–281.
18. Owen M, Friedenstein AJ (1988) Stromal stem cells: Marrow-derived osteogenic precursors. *Ciba Found Symp* 136:42–60.
19. Colter DC, Sekiya I, Prockop DJ (2001) Identification of a subpopulation of rapidly self-renewing and multipotential adult stem cells in colonies of human marrow stromal cells. *Proc Natl Acad Sci USA* 98(14):7841–7845.
20. Kota DJ, Wiggins LL, Yoon N, Lee RH (2013) TSG-6 produced by hMSCs delays the onset of autoimmune diabetes by suppressing Th1 development and enhancing tolerogenicity. *Diabetes* 62(6):2048–2058.
21. Ortiz LA, et al. (2007) Interleukin 1 receptor antagonist mediates the antiinflammatory and antifibrotic effect of mesenchymal stem cells during lung injury. *Proc Natl Acad Sci USA* 104(26):11002–11007.
22. Németh K, et al. (2009) Bone marrow stromal cells attenuate sepsis via prostaglandin E(2)-dependent reprogramming of host macrophages to increase their interleukin-10 production. *Nat Med* 15(1):42–49.
23. English K (2013) Mechanisms of mesenchymal stromal cell immunomodulation. *Immunol Cell Biol* 91(1):19–26.
24. Meisel R, et al. (2004) Human bone marrow stromal cells inhibit allogeneic T-cell responses by indoleamine 2,3-dioxygenase-mediated tryptophan degradation. *Blood* 103(12):4619–4621.
25. Larson BL, Ylostalo J, Lee RH, Gregory C, Prockop DJ (2010) Sox11 is expressed in early progenitor human multipotent stromal cells and decreases with extensive expansion of the cells. *Tissue Eng Part A* 16(11):3385–3394.
26. Foskett AM, et al. (2014) Phase-directed therapy: TSG-6 targeted to early inflammation improves bleomycin-injured lungs. *Am J Physiol Lung Cell Mol Physiol* 306(2): L120–L131.
27. Yamaguchi M, Weitzmann MN (2009) The estrogen 17beta-estradiol and phytoestrogen genistein mediate differential effects on osteoblastic NF-kappaB activity. *Int J Mol Med* 23(2):297–301.
28. Klampfer L, Chen-Kiang S, Vilcek J (1995) Activation of the TSG-6 gene by NF-IL6 requires two adjacent NF-IL6 binding sites. *J Biol Chem* 270(8):3677–3682.
29. Kolenko V, et al. (1999) Inhibition of NF-kappa B activity in human T lymphocytes induces caspase-dependent apoptosis without detectable activation of caspase-1 and -3. *J Immunol* 163(2):590–598.
30. Kratz A, Ferraro M, Sluss PM, Lewandrowski KB (2004) Case records of the Massachusetts General Hospital: Weekly clinicopathological exercises. Laboratory reference values. *N Engl J Med* 351(15):1548–1563.
31. Hay J, Shahzeidi S, Laurent G (1991) Mechanisms of bleomycin-induced lung damage. *Arch Toxicol* 65(2):81–94.
32. Chen GY, Nuñez G (2010) Sterile inflammation: Sensing and reacting to damage. *Nat Rev Immunol* 10(12):826–837.
33. Okin D, Medzhitov R (2012) Evolution of inflammatory diseases. *Curr Biol* 22(17): R733–R740.
34. Oh JY, et al. (2012) Intravenous mesenchymal stem cells prevented rejection of allogeneic corneal transplants by aborting the early inflammatory response. *Mol Ther* 20(11):2143–2152.
35. Verdonk P, Klinge I (2012) Mainstreaming sex and gender analysis in public health genomics. *Gend Med* 9(6):402–410.
36. Martín-Millán M, Castañeda S (2013) Estrogens, osteoarthritis and inflammation. *Joint Bone Spine* 80(4):368–373.
37. Evans J, Salamonsen LA (2012) Inflammation, leukocytes and menstruation. *Rev Endocr Metab Disord* 13(4):277–288.